

Discrete soliton collisions in a waveguide array with saturable nonlinearity

J. Cuevas,¹

*Grupo de Física No Lineal. Departamento de Física Aplicada I., EU Politécnica.
Universidad de Sevilla, C/ Virgen de África, 7, 41011-Sevilla, Spain*

J. C. Eilbeck²

*Department of Mathematics, Heriot-Watt University. Riccarton, Edinburgh, EH14
4AS, UK*

Abstract

We study the symmetric collisions of two mobile breathers/solitons in a model for coupled wave guides with a saturable nonlinearity. The saturability allows the existence of breathers with high power. Three main regimes are observed: breather fusion, breather reflection and breather creation. The last regime seems to be exclusive of systems with a saturable nonlinearity, and has been previously observed in continuous models. In some cases a “symmetry breaking” can be observed, which we show to be an numerical artifact.

Key words:

Solitons, waveguide arrays, saturable nonlinearity

PACS: 42.65.Tg., 05.45.Yv., 42.82.Et

1 Introduction

Since the 1960's, a great number of papers have considered the properties of solitons in nonlinear optic media with a Kerr-type (cubic) nonlinearity. This media can be modelled by the cubic Nonlinear Schrödinger (NLS) Equation. As it is well known, the NLS equation is integrable and, in consequence, solitons interact elastically [1].

¹ Corresponding author. E-mail: jcuevas@us.es

² E-mail: J.C.Eilbeck@hw.ac.uk

More recently, several authors have studied the properties of solitons in photo-refractive media [2]. In this case, the equation describing these media is a modification of the original NLS, which consists in substituting the Kerr non-linearity term by another one of saturable type. This Saturable (SNLS) Equation is nonintegrable and the soliton collision processes are inelastic, leading to annihilation, fusion or creation of solitons [3]. This last phenomena consists of the appearance of three solitons after the collision of only two of them. Another important feature of the SNLS is that the behaviour of the solutions is quite generic, being independent of the details of the mathematical model.

The *discrete* version of the NLS equation can be used to describe nonlinear waveguide arrays within the tight binding approximation [4]. The existence and properties of mobile discrete breathers/solitons in DNLS lattices has been considered in a number of studies (We use the terms breathers and solitons interchangeably in this context, also intrinsic localized modes). An early brief study [5] showed that breathers could propagate along the lattice with a small loss of energy, and could become trapped by inhomogeneities in the lattice. Later, a more detailed study [6] suggested that “exact” travelling breathers might exist, at least for some parameter ranges. The reviews [7,8] refer to many other papers in this area. More recently, work has concentrated on breathers with infinite oscillating tails [9], although the question of the *existence* of *exact* breather solutions which tend to zero as $n \rightarrow \pm\infty$ has not yet been resolved. Given the long history of mobile breather solutions of this equation, it is rather surprising that a systematic study of the collision of two breathers in the DNLS model has only recently been carried out [10]. (We mention also that collisions have been studied in generalised nearly integrable DNLS model in [11,12]).

Recently, some studies have considered the existence of mobile breathers in waveguide arrays in photo-refractive crystal, described by a DNLS equation with saturable nonlinearity [13,14]. In particular, these papers considered a discrete version of the Vinetskii-Kukhtarev model [2,15]. This model system, which we consider in this paper, is governed by the following equation of motion

$$i\dot{u}_n - \beta \frac{u_n}{1 + |u_n|^2} + (u_{n+1} - 2u_n + u_{n-1}) = 0. \quad (1)$$

The key difference between the cubic DNLS equation and the saturable DNLS equation is that in the later, the Peierls–Nabarro barrier (the energy difference between a bond-centred and a site-centred breather with the same power) is bounded and, in most cases, smaller than in the former [16]. It allows the existence of mobile breathers of high power.

It is worth noting that there is another saturable DNLS equation in the liter-

ature, namely

$$i\dot{\psi}_n + \frac{\nu|\psi_n|^2}{1 + \mu|\psi_n|^2}\psi_n + (\psi_{n+1} - 2\psi_n + \psi_{n-1}) = 0. \quad (2)$$

For example, Khare et al. [17] have recently published an exact stationary breather solution for (2), although in fact the stationary solution of this equation is just the solution to an integrable map first published by McMillan in 1971 [18]. Maluckov et al. [19] have also recently studied stationary solutions of (2). However, the two models are not independent, solutions of (2) can be mapped into solutions of (1) by the (invertible) transformation

$$\psi_n(t) = \frac{1}{\sqrt{\mu}} \exp\{i\nu t/\mu\} u_n(t), \quad \beta = \nu/\mu.$$

The aim of the present paper is to study breather-breather collisions in the saturable DNLS equation (1) and to compare the results with those obtained in the continuous SNLS and the discrete cubic equation.

2 Numerical results

This model (1) has two conserved quantities: the Hamiltonian $H = \sum_n [\beta \log(1 + |u_n|^2) + |u_{n-1} - u_n|^2]$ and the power (or norm) $P = \sum_n |u_n|^2$.

In order to reduce the dimension of the large parameter space to be considered, we have fixed β to $\beta = 2$. Higher values of β lead to solutions that only can be moved for a restricted set of power values [13]. Note that the localized stationary breather solution of [17] only exists for $\beta > 2$, and hence are not relevant to our discussions which focus on the $\beta = 2$ case. It would be interesting to extend the calculations in this paper to other values of β to see if the presence of these stationary solutions affected the results given here.

A moving breather $v_n(t)$ is obtained by adding a thrust q to a stationary breather u_n , so that:

$$v_n(0) = u_n \exp(i q n). \quad (3)$$

Notice that this procedure of obtaining moving breathers is similar to the marginal mode method introduced in [20,21] for Klein–Gordon lattices.

In the following, we consider the collision of two identical breathers moving in opposite directions with the same thrust q . Analogously to Ref. [10], we consider both inter-site (IS) and on-site (OS) collisions.

The collision scenario we observe for small P is quite simple: there exists a critical value q_c below which breathers form a bound state, and above which, breathers are reflected (See Fig. 1a-b for examples of these two cases). It can be observed that the bound state “oscillates” after the collision. The amplitude of these oscillations decreases when approaching to the critical point, whereas their “period” increases. (Note that the “reflection” case could equally be regarded as a transmission case as the two breathers are indistinguishable. In the case of reflection/transmission, there is some loss of energy of the two breathers).

For high values of P , the above scenario takes place, except that, for high values of q , *breather creation* is observed. Figure 1c shows an example of such a collision. This behaviour is similar to the soliton creation observed in the saturable continuous models and will be analyzed in more detail below. The different regimes in the (P, q) plane are depicted in Figure 2, for both IS and OS collisions. Furthermore, Fig. 3 shows the values of the critical value of q separating merging and reflecting regimes, as a function of the power P . It can be seen that, for most choices of P , both values are close. This is different from the cubic DNLS case [10] where the critical values of the OS case is an order of magnitude higher than the ones for the IS case. The likely explanation is that in the saturable case, the PN barrier is small (for our choice $\beta = 2$, the absolute value of the barrier is smaller than 0.01).

For high values of P , we have also observed the merging of two breathers with symmetry breaking, as reported in [10]. This symmetry breaking manifests as a movement of the final bound state to left or to the right accompanied by the appearance of a total lattice momentum, defined by $p = i \sum_n (\psi_{n+1} \psi_n^* - \psi_{n+1}^* \psi_n)$. Since the equation, the initial conditions, and the boundary conditions are symmetric, this state must be a numerical artifact, as suggested in [10]. To test this hypothesis further, we performed some runs with either (a) increased numerical accuracy in the numerical integration routines, or (b), the addition of some very small random noise to the initial conditions. In case (a), the onset of symmetry breaking is shifted to longer times, whereas in case (b), symmetry breaking is observed at shorter times. These numerical results confirm that symmetry breaking is a numerical artifact caused by random rounding errors breaking the symmetry of the problem. However these “spurious” results are interesting in their own right as they suggest that at these higher values of P , the stationary breather formed after collision is more easily set into motion by a very small perturbation. To check that the other phenomena we observe is *not* due to numerical artifacts, we have carried out similar tests on other runs showing different phenomena. No such sensitivity to random errors of the accuracy of the integrators is observed.

3 Breather creation

We proceed to analyze the breather creation process, as it is most noteworthy phenomenon that appears in the saturable case in comparison to the cubic one. From Figs. 2 and 4 we can conclude that the conditions for breather creation are that P and q are above a threshold value.

This result can be explained with the aid of Fig. 5, where the density power of the collision point, for the cases of reflection and breather creation, is shown. It can be seen that the power density oscillates after the collision, and its minimum is zero for the case of no creation. The minimum power density after the collision for all the simulations (neglecting the trapping regime) is represented in Fig. 4. In consequence, the trapped power must be above a threshold so that breather creation occurs. It can be explained by the fact that, for a stationary breather to have a “saturable” behaviour, its power should be higher than a threshold value. This phenomenon is similar to the soliton bistability observed for SNLS solitons in [22]. It consists of the existence of a minimum in the dependence of the soliton width with respect to the peak intensity. This dependence is monotonically decreasing in the cubic NLS, and thus the soliton in a saturable medium has a Kerr behaviour for small peak intensities (or power). In the discrete case, as the width is less well-defined, we have considered instead $W = |u_1|^2/|u_0|^2$, where $n = 0$ is chosen as the centre (or peak) of the breather. Fig. 6 shows W versus P displaying a similar behaviour as in the continuous case.

The analysis given above also explain why the results of [10] (i.e. only merge and reflection regimes take place) are found for small values of the power. We note also that this creation process may be related to the phenomena of the fission of a coupled two-breather state into a stationary and a moving breather in the DNLS equation [21].

4 Effect of phase in breather collisions

To complete the paper, we give a brief study of the effect of considering a phase difference between the breathers, in a similar fashion to Ref. [11]. This is achieved by introducing a factor $\exp(i\phi)$ in one of the breathers. Fig. 7 shows the final amplitudes $A_{1,2}$ and velocities $V_{1,2}$ of both breathers as a function of ϕ .

It appears that the final velocities are smooth functions of ϕ , showing a strong phase effect, with the V_2 curve following the V_1 curve, phase-shifted by π . The V values vary from around 0.2 to 0.8. The amplitude dependence, on the

other hand, is much smaller but shows a much more irregular behaviour as a function of ϕ . Clearly the discreteness of the lattice is featuring strongly here in this latter case.

Finally, in Fig. 8, we show the relation between the outgoing velocities as ϕ varies through 2π , analogously to Fig. 3 of [11]. Here the relatively smooth behaviour over a large range of V values is clearly shown.

5 Conclusions

We have analyzed the collisional behaviour in a saturable DNLS model, finding close analogies to the continuous NLS equation. Breathers can merge, reflect or be created (although breather annihilation is not observed). The extra power available to breathers in the SDNLS case results in the new phenomena of breather creation in a discrete model. Additionally, the scenario in the saturable DNLS case seems to be much “cleaner” than in the cubic DNLS case on a coarse scale, with a strong but simpler threshold effect. These facts may be an advantage in some applications, such as multi-port optical switching. There are still a number of details in the fine-scale structure which are as yet unexplained. These may perhaps be understood through the application of a future variational study. It would also be interesting to extend this study to consider the collision of two non-identical breathers.

6 Acknowledgements

One of us (JC) acknowledges financial support from the MECD/FEDER project FIS2004-01183. The other (JCE) would like to acknowledge the hospitality of the University of Seville for hosting research visits during which this work was discussed.

References

- [1] V. E. Zakharov, and A. B. Shabat. *Sov. Phys. JETP*, 34:62, 1972.
- [2] W. Królikowski, B. Luther-Davies, and C. Denz. *IEEE J. Quantum Electron.*, 39:3, 2003.
- [3] S. Cowan, et al. *Can. J. Phys.*, 64:311, 1986; A. W. Snyder, and A. P. Sheppard. *Opt. Lett.*, 18:482, 1993; W. Królikowski, and S. A. Holmstrom. *Opt. Lett.*,

- 22:369, 1997; M. H. Jakubowski, K. Steiglitz, and R. Squier. *Phys. Rev. E*, 56:7276, 1997.
- [4] D. N. Christodoulides, F. Lederer, and Y. Silberberg. *Nature*, 424:817, 2003.
- [5] J. C. Eilbeck. In Chikao Kawabata and A. R. Bishop, eds., *Computer Analysis for Life Science – Progress and Challenges in Biological and Synthetic Polymer Research*, pp. 12–21, Tokyo, 1986. Ohmsha.
- [6] H. Feddersen. In M. Remoissenet and M. Peyrard, eds., *Nonlinear coherent structures in physics and biology, Lecture notes in physics* **393**, pp. 159–167. Springer, 1991.
- [7] J. C. Eilbeck and Magnus Johansson. In L. Vázquez, R. S. MacKay, and M. P. Zorzano, eds., *Localization and Energy Transfer in Nonlinear Systems*, pp. 44–67, Singapore, 2003. World Scientific.
- [8] P. G. Kevrekidis, K. Ø. Rasmussen, and A. R. Bishop. *Int. J. Mod. Phys. B*, 15:2833, 2001.
- [9] J. Gómez-Gardeñes, F. Falo, and L. M. Floría. *Phys. Lett. A*, 332:213, 2004.
- [10] I. E. Papacharalampous, et al. *Phys. Rev. E*, 68:046604, 2003.
- [11] S. V. Dmitriev, et al. *Phys. Rev. E*, 68:056603, 2003.
- [12] D. Cai, A. R. Bishop, and N. Grønbech-Jensen. *Phys. Rev. E*, 56:7246, 1997.
- [13] L. Hadzievski, et al. *Phys. Rev. Lett.*, 93:033901, 2004.
- [14] M. Stepic, et al. *Phys. Rev. E*, 69:066618, 2004.
- [15] V. O. Vinetskii, and N. V. Kukhtarev. *Sov. Phys. Solid State*, 16:2414, 1975.
- [16] Yu. S. Kivshar, and D. K. Campbell. *Phys. Rev. E*, 48:3077, 1993.
- [17] A. Khare, et al. *J. Phys. A*, 38:807, 2005.
- [18] E. M. McMillan. In W. E. Brittin and H. Odabasi, eds., *Topics in Modern Physics: A Tribute to E. U. Condon*, pages 219–244, Colorado Associated Univ. Press:Boulder, 1971.
- [19] A. Maluckov et al., *Eur. Phys. J. B* 45:539, 2005.
- [20] Ding Chen, S. Aubry, and G. P. Tsironis. *Phys. Rev. Lett.*, 77:4776, 1996.
- [21] S. Aubry and T. Cretegny. *Physica D*, 119:34, 1998.
- [22] W. Królikowski, et al. *Phys. Rev. E*, 61:2010, 2000.

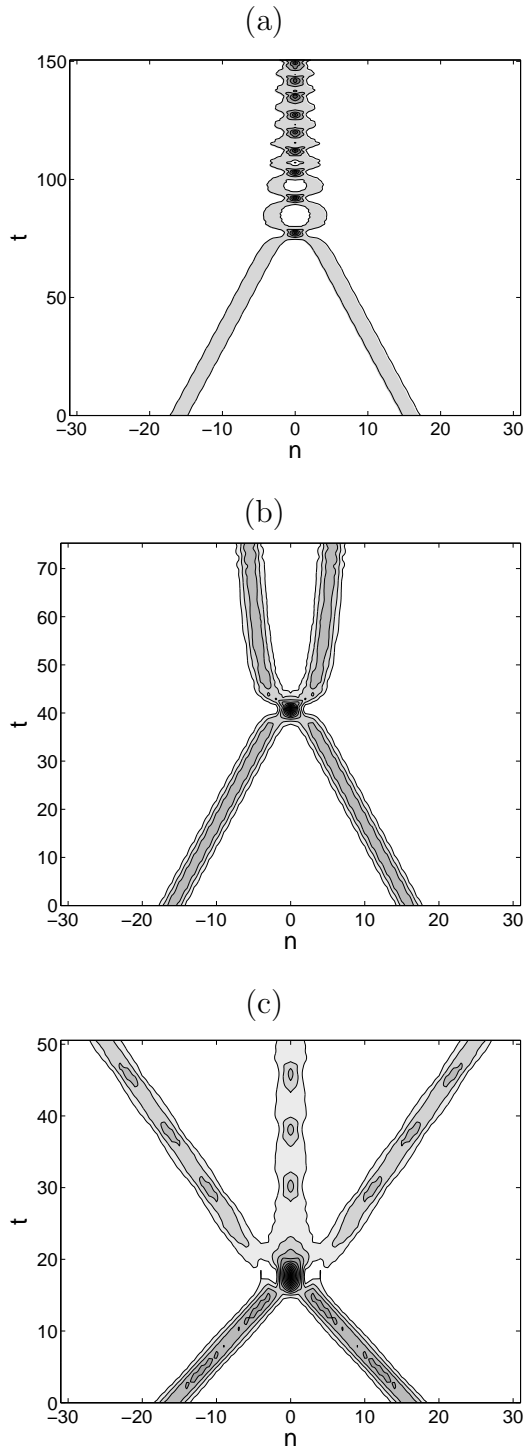


Fig. 1. Typical power density plots for (a) bound state formation ($P = 10, q = 0.1$), (b) reflection ($P = 10, q = 0.2$), and (c) breather creation ($P = 70, q = 0.5$). In all cases, OS collisions are considered, although these pictures do not vary considerably for IS collisions.

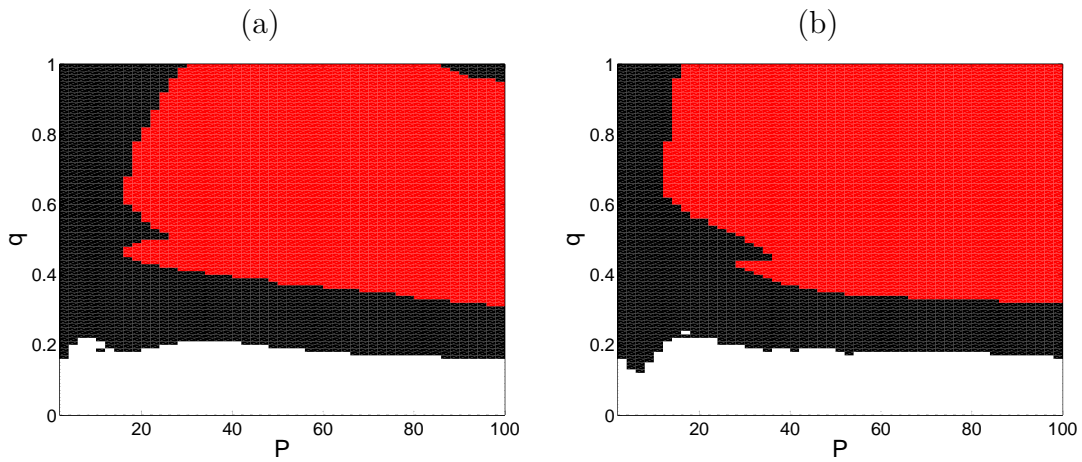


Fig. 2. Different regimes observed in (a) IS and (b) OS collisions. The colours represent the following: white-merge to a single breather; black-reflection; and red-breather creation

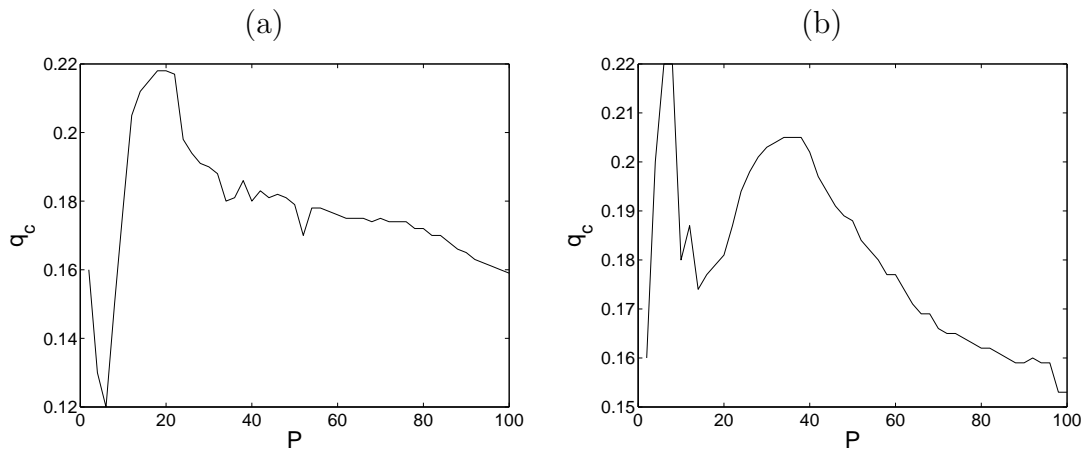


Fig. 3. Critical value of the initial thrust q for (a) IS and (b) OS collisions versus P .

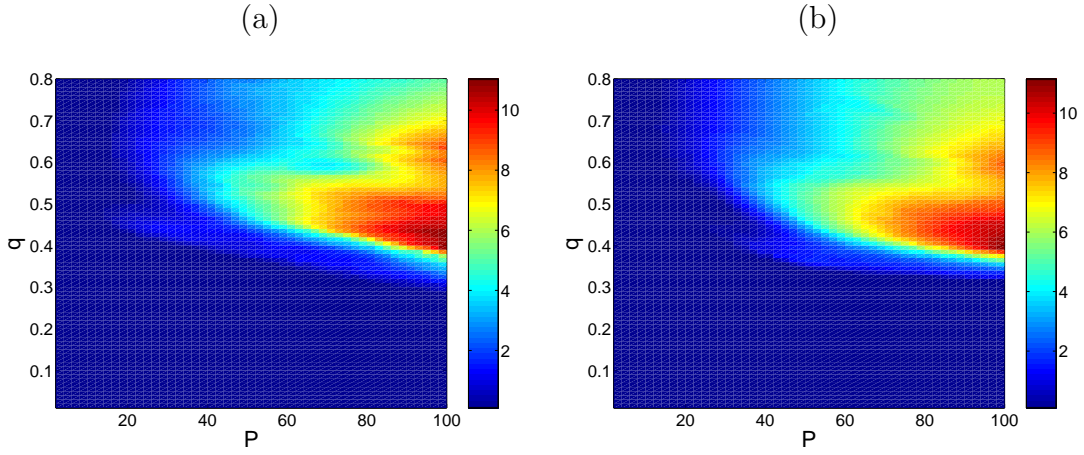


Fig. 4. Minimum value of the power density at the collision point after collision as a function of P and q . Left (right) panel corresponds to inter-(on-) site collisions. We have supposed that the power trapped in the trapping regime is zero in order to clarify the figure.

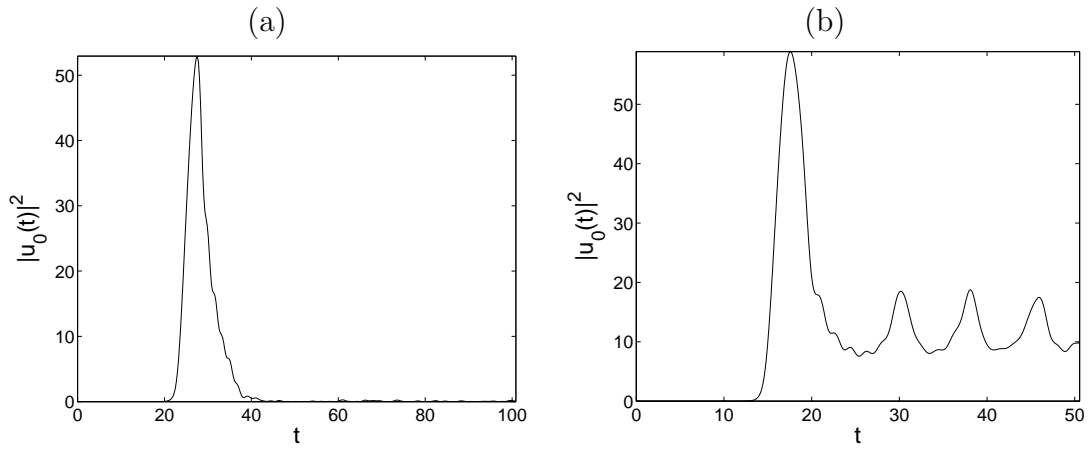


Fig. 5. Time evolution of the power density at the collision point ($|u_0|^2$). The left panel corresponds to a reflection case ($q = 0.3$, $P = 70$) and the right panel to a creation case ($q = 0.7$, $P = 70$).

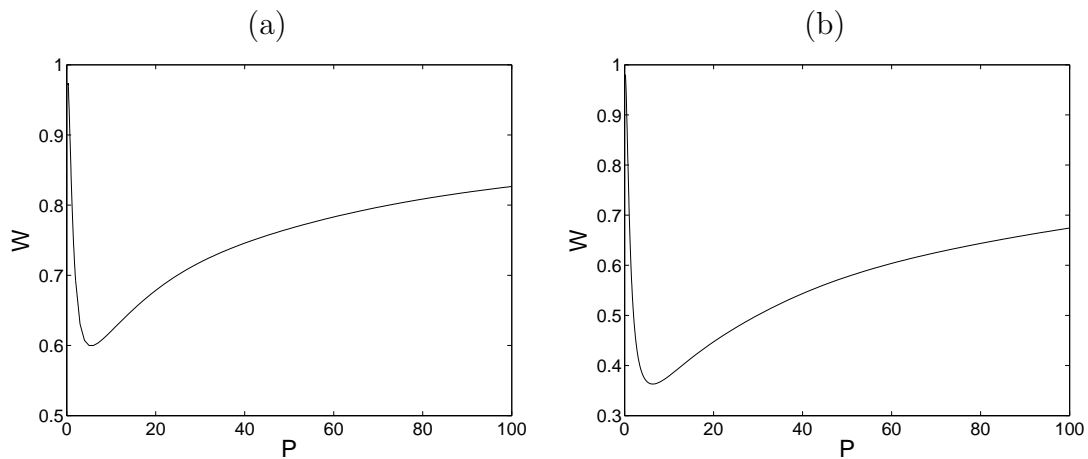


Fig. 6. Representation of the “breather width” W (defined as $W = |u_1|^2/|u_0|^2$) versus the power of a stationary site-centred (left) and a bond-centred (right) breather.

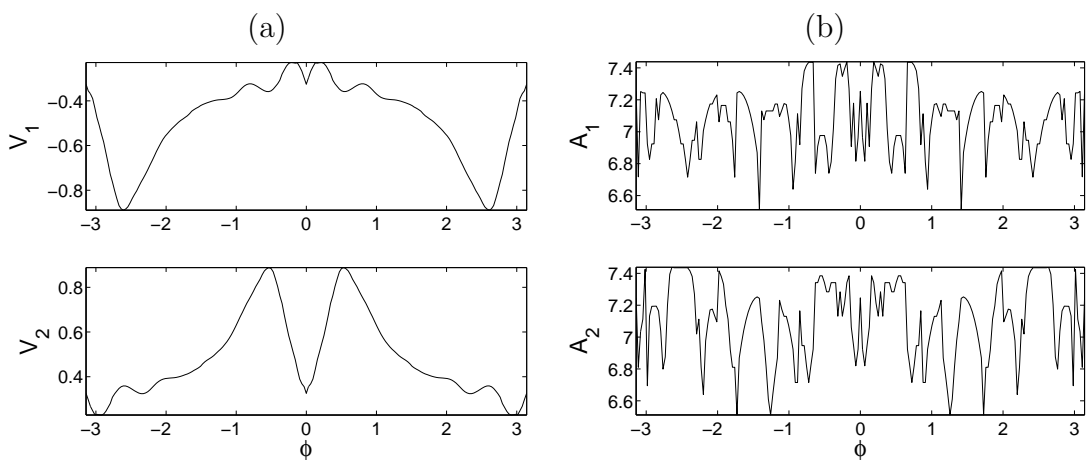


Fig. 7. Final velocities (a) and amplitudes (b) with respect to the phase for breathers with $P = 20$ and $q = 0.25$ and an OS collision.

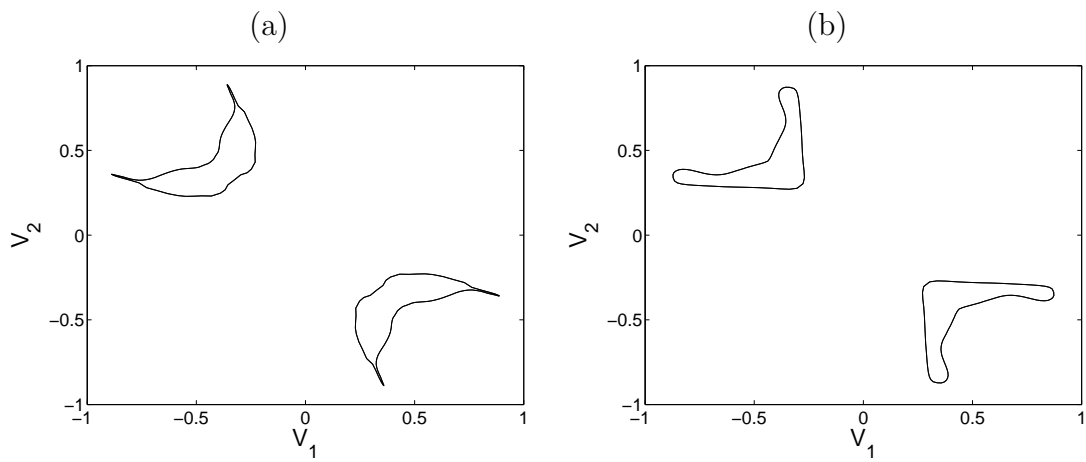


Fig. 8. Relation between the final velocities for breathers with $q = 0.25$ and (a) $P = 20$; (b) $P = 10$. OS collisions are considered in both cases